

The putative G protein–coupled receptor Gr1D mediates extracellular polyphosphate sensing in *Dictyostelium discoideum*

Patrick M. Suess[†], Yu Tang, and Richard H. Gomer^{*}

Department of Biology, Texas A&M University, College Station, TX 77843-3474

ABSTRACT Five or more orthophosphates bound together by high-energy phosphoanhydride bonds are highly ubiquitous inorganic molecules called polyphosphate. Polyphosphate acts as a signaling molecule eliciting a number of responses in eukaryotic cells, but the mechanisms mediating these effects are poorly understood. Proliferating *Dictyostelium discoideum* cells accumulate extracellular polyphosphate. At extracellular concentrations similar to those observed in stationary phase cells, polyphosphate inhibits proteasome activity and proliferation, and induces aggregation. Here we identify Gr1D as a putative G protein–coupled receptor that mediates binding of extracellular polyphosphate to the cell surface. Cells lacking Gr1D do not respond to polyphosphate-induced proteasome inhibition, aggregation, or proliferation inhibition. Polyphosphate also elicits differential effects on cell–substratum adhesion and cytoskeletal F-actin levels based on nutrient availability, and these effects were also mediated by Gr1D. Starving cells also accumulate extracellular polyphosphate. Starved cells treated with exopolyphosphatase failed to aggregate effectively, suggesting that polyphosphate also acts as a signaling molecule during starvation-induced development of *Dictyostelium*. Together, these results suggest that a eukaryotic cell uses a G protein–coupled receptor to mediate the sensing and response to extracellular polyphosphate.

Monitoring Editor

Carole Parent
University of Michigan

Received: Oct 30, 2018

Revised: Jan 18, 2019

Accepted: Feb 14, 2019

INTRODUCTION

Polyphosphate is a simple inorganic molecule found throughout nature, consisting of linear chains of phosphates linked by high-energy phosphoanhydride bonds (Brown and Kornberg, 2004). In prokaryotes, where the majority of polyphosphate studies have occurred, polyphosphate is synthesized by the highly conserved bacterial enzyme polyphosphate kinase, and has roles in a myriad of cellular functions, such as growth, survival in stationary phase, stress endurance, quorum sensing, phosphate storage, heavy metal resistance, and virulence (Rao and Kornberg, 1996; Rao et al., 2009; Rashid et al., 2000; Achbergerova and Nahalka, 2011; Gray and

Jakob, 2015; Kulakovskaya, 2018). Polyphosphate is a component of the cell wall in various fungi and algae (Werner et al., 2007a,b), whereas in eukaryotes polyphosphate has been identified in subcellular locations such as the nuclei, mitochondria, and the plasma membrane (Kumble and Kornberg, 1995). Polyphosphate has roles in inflammation, blood coagulation, proliferation, biomineralization, osteogenic differentiation, and apoptosis (Wang et al., 2003; Kawano, 2006; Smith et al., 2006; Morrissey et al., 2012; Ozeki et al., 2015; Ardeshirylajimi et al., 2018; Kato et al., 2018), but the mechanism by which polyphosphate elicits its various cellular responses in eukaryotes is largely unknown.

Dictyostelium discoideum is a eukaryotic social amoeba that accumulates extracellular polyphosphate, which then acts as an autocrine signaling molecule (Suess and Gomer, 2016), as well as intracellular polyphosphate, which plays a role in growth, fitness, germination, and development (Livermore et al., 2016). Extracellular polyphosphate inhibits proliferation of high-cell-density cultures through an autocrine negative feedback mechanism, inducing a stationary phase of proliferation. In addition, we found that polyphosphate inhibits the proteasome activity of *Dictyostelium* cells through a pathway mediated by Ras and Akt, which primes cells for the transition from vegetative growth to differentiation and development,

This article was published online ahead of print in MBoC in Press (<http://www.molbiolcell.org/cgi/doi/10.1091/mbc.E18-10-0686>) on February 20, 2019.

[†]Present address: University of Michigan Medical School, 1150 W. Medical Center Dr., Ann Arbor, MI 48109-0600.

^{*}Address correspondence to: Richard H. Gomer (rgomer@tamu.edu).

Abbreviations used: PolyP, polyphosphate; PPX1, exopolyphosphatase.

© 2019 Suess et al. This article is distributed by The American Society for Cell Biology under license from the author(s). Two months after publication it is available to the public under an Attribution–Noncommercial–Share Alike 3.0 Unported Creative Commons License (<http://creativecommons.org/licenses/by-nc-sa/3.0>).

“ASCB®,” “The American Society for Cell Biology®,” and “Molecular Biology of the Cell®” are registered trademarks of The American Society for Cell Biology.

and induces aggregation as cells approach starvation (Suess *et al.*, 2017). Cells lacking RasC (Daniel *et al.*, 1994) or both *Dictyostelium* Akt homologues PkbA and PkgB (Meili *et al.*, 2000) are unresponsive to several polyphosphate responses, including aggregation, proteasome inhibition, and increased expression of the developmental gene *csA* (Suess *et al.*, 2017). Intriguingly, polyphosphate also inhibits proteasome activity and proliferation of several human leukemia cell lines, suggesting that this effect is at least conserved from *Dictyostelium* to humans (Suess *et al.*, 2017). Cells lacking inositol hexakisphosphate kinase, which uses IP6 as a substrate to generate the inositol pyrophosphates IP7 and IP8, have diminished extracellular polyphosphate accumulation in *D. discoideum* (Suess and Gomer, 2016). This link between inositol hexakisphosphate kinase and polyphosphate accumulation has also been observed in yeast and murine platelets (Auesukaree *et al.*, 2005; Ghosh *et al.*, 2013), marking the first conserved component identified as having a role in polyphosphate accumulation in eukaryotes.

Dictyostelium responds to a number of extracellular signaling molecules and stimuli, such as cAMP which acts as a chemoattractant during development, through G protein-coupled receptors (GPCRs; Prabhu and Eichinger, 2006). The *Dictyostelium* genome encodes 61 putative GPCRs, including 17 GABA_B or metabotropic glutamate receptor-like proteins, known as Grl (glutamate receptor-like) proteins (Heidel *et al.*, 2011). In this article, we identify the putative metabotropic glutamate receptor-like protein GrlD as a mediator of the extracellular polyphosphate binding as well as polyphosphate-induced proteasome inhibition, proliferation inhibition, and changes in cell-substratum adhesion and the actin cytoskeleton.

RESULTS

GrlD mediates aggregation induced by extracellular polyphosphate and polyphosphate binding

In low nutrient conditions as *Dictyostelium* cells approach starvation, polyphosphate can initiate aggregation, the first stage of development (Suess *et al.*, 2017). Polyphosphate binds to *Dictyostelium* cells

(Suess and Gomer, 2016), so to identify a potential cell-surface polyphosphate receptor, we screened a collection of receptor mutants for abnormal polyphosphate-induced aggregation in low nutrient conditions. We previously found that mutations in the genes encoding the putative receptors FslB, FslK, GrlB, GrlE, and GrlH did not affect polyphosphate-induced aggregation (Suess *et al.*, 2017). We found that cells lacking the GPCR GrlD (*grlD*⁻ cells) were unresponsive to polyphosphate-induced aggregation (Figure 1A). GrlD is one of 17 putative metabotropic glutamate receptor-like proteins in *Dictyostelium* (Prabhu and Eichinger, 2006). *grlD*⁻ cells proliferate slower than wild type, accumulate abnormally high levels of the secreted proteins AprA and CfaD, tend to have more nuclei per cell than wild type, are unresponsive to proliferation inhibition by recombinant CfaD, and are unresponsive to recombinant AprA proliferation inhibition and chemorepulsion (Tang *et al.*, 2018). Wild-type cells show saturable binding to biotinylated polyphosphate (Suess and Gomer, 2016), whereas cells lacking GrlD did not have any detectable binding (Figure 1B). These data suggest that GrlD is a putative extracellular polyphosphate receptor. The binding kinetics of polyphosphate to *Dictyostelium* cells was slightly different from what was previously observed (Suess and Gomer, 2016). This may be due to slight differences in the size distribution of the biotinylated polyphosphate, which is produced as a heterologous mixture of sizes with a mean length of 100 residues, and size differences have been shown to affect the binding to *Dictyostelium* (Suess and Gomer, 2016). To verify the phenotype of the *grlD*⁻ cells, *grlD* mRNA was expressed under the control of the constitutively active actin 15 promoter in the *grlD*⁻ background, creating *grlD*⁻/a15::*grlD* cells. These cells showed expression of the *grlD* transcript as determined by reverse transcription PCR (RT-PCR), but with *grlD* mRNA levels higher than observed in wild-type cells (Supplemental Figure S1A). The expression of *grlD* in the *grlD*⁻ cells rescued an abnormal developmental phenotype (generally no observable aggregates, with occasional misformed structures) observed in the *grlD*⁻ cells for cells grown on lawns of bacteria on agar, while only a partial rescue was observed

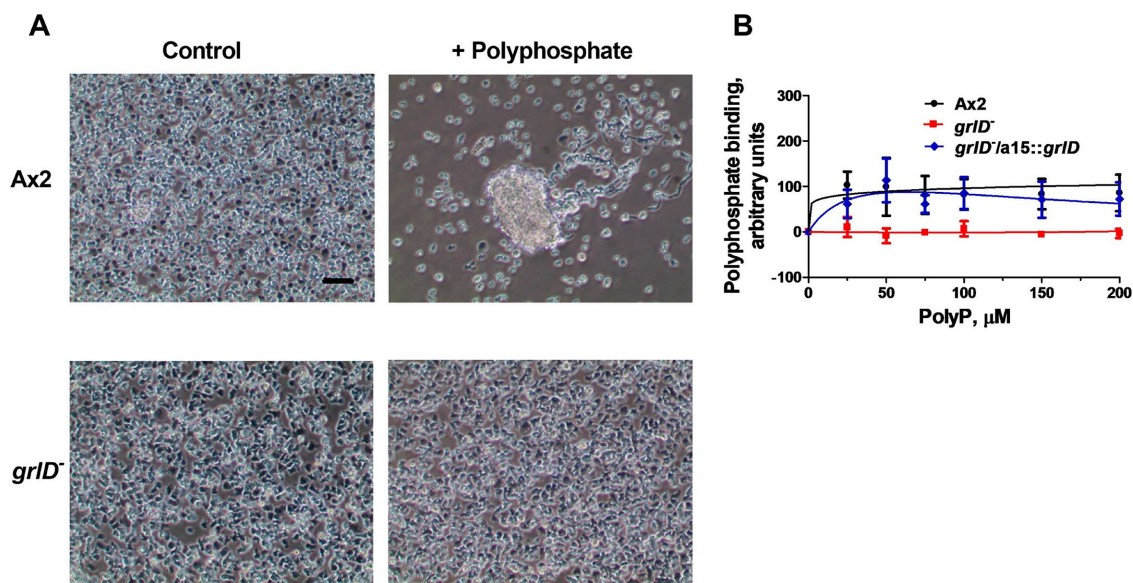


FIGURE 1: GrlD is a putative polyphosphate receptor. (A) Cells were grown in 25% HL5 in submerged nonshaking culture in the presence or absence of 150 µM polyphosphate (polyP) for 24 h. Images are representative of seven independent experiments. Bar is 50 µm. (B) The indicated cell lines were incubated with the indicated amounts of biotinylated polyphosphate and streptavidin-conjugated fluorophore. The cells were washed, and fluorescence was measured using a flow cytometer. Values are mean ± SEM, *n* = 3. Lines are curve fits to specific binding with variable Hill slope.

for cells developed on nitrocellulose filter pads (Supplemental Figure S1, B and C). Expression of *grlD* in the *grlD*⁻ cells rescued polyphosphate binding (Figure 1B). To determine whether cells lacking GrlD have altered expression of the early onset developmental gene discoidin (Frazier *et al.*, 1975), vegetative and starved cells were stained for discoidin. Cells lacking GrlD showed positive discoidin staining after 2 h starvation, suggesting that these cells have some of the machinery necessary for the transition from vegetative growth to development (Supplemental Figure S1D). Expression of *grlD* in the *grlD*⁻ cells did not rescue polyphosphate-induced aggregation in submerged cultures when HL5 was present, but did rescue starvation-induced aggregation in submerged cultures (Supplemental Figure S1E). One possible explanation for the ability of overexpressing *grlD* in *grlD*⁻ cells to rescue, in submerged cultures, starvation-induced aggregation but not polyphosphate-induced aggregation in low nutrients is that high levels of *grlD* mRNA may enhance nutrient sensing, thereby inhibiting aggregation in the presence of even very low nutrients. Together, these results suggest that GrlD is required for cells to bind and sense polyphosphate.

To determine the ability of cells lacking GrlD to obtain aggregation competence upon the induction of starvation, quantitative PCR (qPCR) and semiquantitative RT-PCR were performed after 0, 4, 8, and 12 h of starvation to detect markers of starvation-induced cAMP signaling and aggregate formation (Loomis, 2014). As previously observed, wild-type cells showed development-induced increases in mRNAs encoding the cell-surface glycoprotein CsaA (Noegel *et al.*, 1986), the cAMP receptor Car1 (Ginsburg *et al.*, 1995), and the adenyl cyclase AcaA (Supplemental Figure S2, A–E; Pitt *et al.*, 1992). Cells lacking GrlD showed development-induced increases in these mRNAs, but to levels lower than in wild-type cells (Supplemental Figure S2, A–E). These data suggest that cells lacking GrlD have defects in becoming aggregation competent upon starvation.

Polyphosphate inhibits proliferation in a variety of nutrient conditions

We previously found that polyphosphate induces aggregation in 25% HL5 (Suess *et al.*, 2017). SIH is a synthetic minimal media that facilitates vegetative growth during axenic proliferation. Cells cultured in SIH proliferate to high cell densities in shaking culture, but at slower rates relative to HL5 (Lu *et al.*, 2004). The ability of SIH to maintain vegetative growth in submerged, nonshaking conditions has yet to be explored. To determine whether polyphosphate-induced aggregation also occurs in SIH, we cultured cells in SIH for 24 h with or without polyphosphate. Wild-type cells treated with polyphosphate formed aggregates, whereas untreated cells did not (Figure 2A). As in 25% HL5 (Figure 1A; Suess *et al.*, 2017), cells lacking GrlD, RasC, or PkbA/PkgB were unresponsive to polyphosphate-induced aggregation (Figure 2A). These results indicate that in a second condition, polyphosphate induces aggregation, and that GrlD, RasC, and PkbA/PkgB are required for this process.

Because the accumulation and effects of extracellular polyphosphate are affected by nutrient availability (Suess and Gomer, 2016; Suess *et al.*, 2017), we examined the effects of polyphosphate on the proliferation of wild-type and mutant cells in high and low nutrient conditions. HL5 is a complex, nutrient-rich broth used to culture *Dictyostelium* cells (Soll *et al.*, 1976). 100% HL5 serves as a high nutrient condition, whereas diluted HL5 (25%) serves as a low nutrient condition. Compared to wild type, cells lacking GrlD had a higher doubling time in 100% HL5, cells lacking RasC had a lower doubling time in 25% HL5, and cells lacking Akt had a higher doubling time in 100 and 25% HL5 (Supplemental Figure S3A). As previously observed (Suess and Gomer, 2016), polyphosphate

inhibited proliferation of wild-type cells in 100% HL5 (Figure 2B and Supplemental Table S1A). Cells lacking GrlD showed a reduced response to 150 μ M and higher concentrations of polyphosphate, whereas cells lacking RasC or Akt had a proliferation response to polyphosphate similar to that of wild type (Figure 2B and Supplemental Table S1A). In 25% HL5 or SIH, physiological levels of polyphosphate (150 μ M and lower) reduced the proliferation of wild-type cells but not *grlD*⁻ or *rasC*⁻ cells (Figure 2, C and D, and Supplemental Table S1A). Expression of *grlD* in *grlD*⁻ cells rescued the abnormal response to polyphosphate proliferation inhibition in low nutrients (Supplemental Figure S3, B and C). *grlD7a15::grlD* cells also had abnormally high doubling times relative to both *Ax2* and *grlD*⁻, suggesting that high levels of *grlD* mRNA inhibit proliferation (Supplemental Figure S3D). Compared to wild type, cells lacking both Akt homologues had a slightly reduced proliferation inhibition response to polyphosphate in 25% HL5 and a normal response in SIH (Figure 2, C and D, and Supplemental Table S1A). Together, the data indicate that in high nutrients, GrlD partially mediates proliferation inhibition by polyphosphate, whereas RasC and Akt are not necessary for this effect. In low nutrient conditions, GrlD and RasC are necessary for proliferation inhibition by polyphosphate, whereas Akt is not. These results suggest that polyphosphate inhibits proliferation by two different mechanisms depending on nutrient availability.

Polyphosphate-induced aggregation is dependent not only on nutritional availability, but also local cell density, as low-cell-density cultures did not aggregate in response to polyphosphate under any condition examined (Suess *et al.*, 2017). To determine whether proliferation inhibition by polyphosphate is also affected by cell density, we cultured cells at 0.25×10^6 cells/ml, six times lower than what we used for the experiments described above. Compared to wild-type cells, cells lacking GrlD or Akt had slightly higher doubling times in 100% HL5, whereas cells lacking RasC had a higher doubling time in SIH (Supplemental Figure S3E). In 100% HL5, polyphosphate inhibited low density *Ax2* cells similar to the inhibition observed at high cell densities (Figure 2E and Supplemental Table S1B). The proliferation of cells lacking GrlD, RasC, or Akt was also inhibited by polyphosphate at low cell densities in high nutrient conditions. In low nutrient conditions, the proliferation of wild-type cells was inhibited by polyphosphate at low cell densities; however, in 25% HL5 the IC50 was higher than at high cell densities (Figure 2, F and G, and Supplemental Table S1B). Cells lacking GrlD or RasC had a normal response to polyphosphate proliferation inhibition at low cell densities in low nutrients (Figure 2, E and G, and Supplemental Table S1B). In 100 and 25% HL5, cells lacking Akt showed an abnormally strong inhibition of proliferation in response to polyphosphate (Figure 2, E and F, and Supplemental Table S1B). Together, these data suggest that GrlD mediates polyphosphate inhibition of proliferation at high but not low cell densities, that RasC mediates this inhibition only at high cell densities in low nutrients, and that at low cell densities in 100 and 25% HL5, Akt counteracts the effects of polyphosphate.

Proteasome activity inhibition inhibits proliferation in low nutrient conditions

We previously found that proteasome inhibition by polyphosphate is linked to the induction of aggregation, and that RasC is necessary for this effect (Suess *et al.*, 2017). To determine whether GrlD is needed for polyphosphate inhibition of proteasome activity, we incubated wild type and cells lacking GrlD with physiological concentrations (150 μ M) of polyphosphate (Suess and Gomer, 2016) and measured proteasome activity. Cells lacking GrlD were unresponsive to polyphosphate-induced proteasome inhibition (Figure 3, A and B).

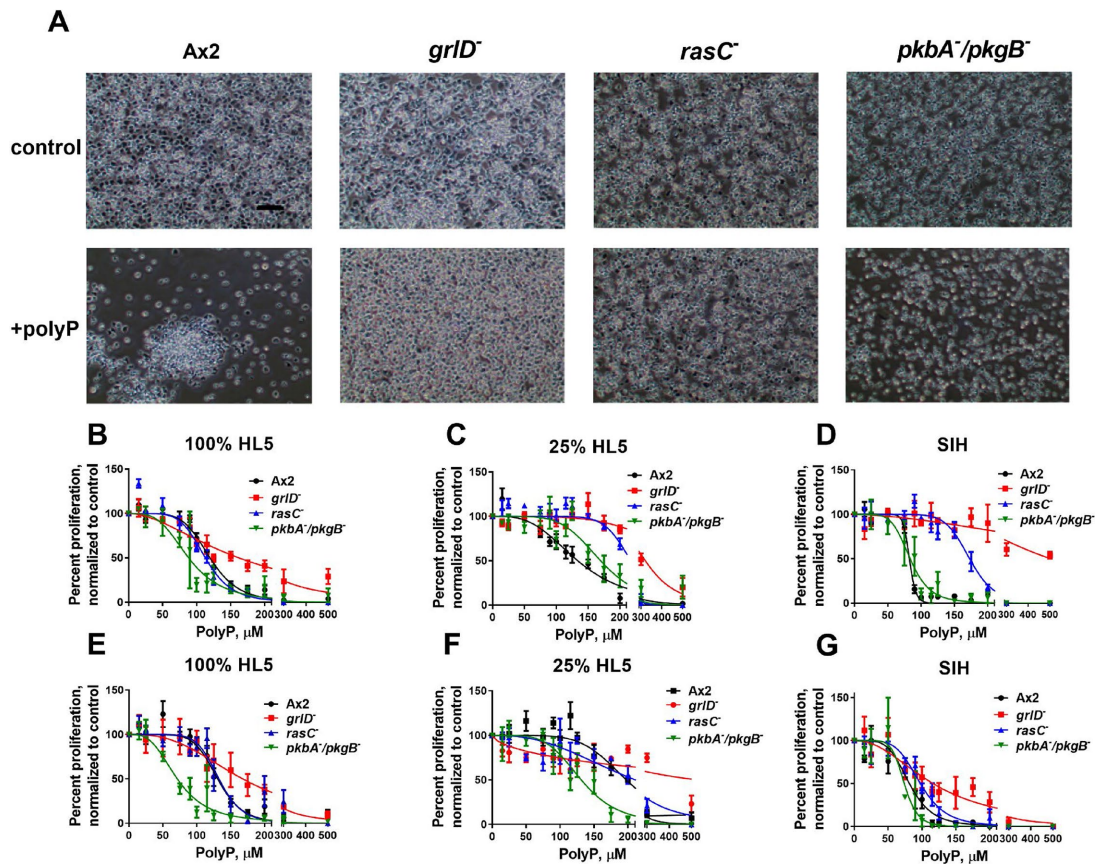


FIGURE 2: Nutrients and cell density affect polyphosphate inhibition of proliferation. (A) The indicated strains were grown in SIH in submerged nonshaking culture in the presence or absence of 150 μM polyphosphate for 24 h. Images are representative of seven independent experiments. Bar is 50 μm . (B–D) The indicated cell lines were grown in submerged nonshaking cultures starting at 1.5×10^6 cells/ml and incubated with the indicated concentrations of polyphosphate in the indicated medium. After 24 h, cell counts were normalized to the no-polyphosphate controls. Absolute values (in units of 10^6 cells/ml) for untreated Ax2 cells were 3.5 ± 0.1 in 100% HL5, 3.6 ± 0.2 in 25% HL5, and 3.3 ± 0.1 in SIH. (E–G) The assays shown in B–D were repeated using cultures with a starting density of 2.5×10^5 cells/ml. Absolute values (in units of 10^5 cells/ml) of untreated Ax2 cells were 1.3 ± 0.1 in 100% HL5, 0.9 ± 0.1 in 25% HL5, and 0.67 ± 0.04 in SIH. All values are mean \pm SEM, $n \geq 3$. Curves are fits to sigmoidal inhibitor responses with variable Hill coefficient.

Because *grlD*⁻ and *rasC*⁻ cells were unresponsive to polyphosphate proliferation inhibition in low nutrient conditions and are also unresponsive to polyphosphate proteasome inhibition, we next assessed whether altered nutrient levels affect polyphosphate-induced proteasome inhibition. Polyphosphate inhibited proteasome activity of wild-type cells in both high and low nutrient conditions, whereas cells lacking GrlD, RasC, or Akt were unresponsive to polyphosphate proteasome inhibition in all conditions (Figure 3, A–D). We previously found that in high nutrient conditions, proteasome inhibition by MG132, a chemical inhibitor of the proteasome (Figure 3, A–D), was unable to inhibit proliferation (Rock *et al.*, 1994; Suess *et al.*, 2017). However, in low nutrient conditions proteasome inhibition by MG132 was sufficient to inhibit proliferation of wild-type cells, as well as all three mutant cell lines (Figure 3, E–H). This suggests that in low nutrient conditions, polyphosphate may inhibit proliferation by inhibiting proteasome activity, whereas in high nutrient conditions, polyphosphate inhibits proliferation by an unknown mechanism. There were no statistically significant differences between Ax2, *grlD*⁻, and *rasC*⁻ basal proteasome activity levels in any nutrient condition; however, *grlD*⁻ cells show a trend for decreased basal proteasome activity in all conditions (Supplemental Figure S4,

A–C). Cells lacking Akt had significantly lower proteasome activity relative to Ax2 in all conditions (Supplemental Figure S4, A–C). MG132 did not inhibit wild type proliferation at low cell densities in high nutrient conditions but did inhibit proliferation at low densities in low nutrient conditions (Supplemental Figure S4D). Cells lacking GrlD, RasC, or Akt at low cell densities were sensitive to MG132-induced proliferation inhibition in all nutrient conditions (Supplemental Figure S4, E–G). Polyphosphate (150 μM) did not inhibit proteasome activity of wild-type or *grlD*⁻ cells at low cell densities regardless of the nutrient condition, suggesting that proliferation inhibition by polyphosphate at low cell densities is not due to decreased proteasome activity (Supplemental Figure S4, H and I).

Like polyphosphate, MG132 can induce aggregation of wild-type cells when cultured in 25% HL5, whereas cells lacking RasC or Akt are unresponsive (Suess *et al.*, 2017). To determine whether cells lacking GrlD are unresponsive to MG132-induced aggregation, we cultured wild-type and *grlD*⁻ cells in 25% HL5 in the presence or absence of MG132. Cells lacking GrlD were unresponsive to MG132-induced aggregation (Supplemental Table S2). This suggests that GrlD may be involved in the aggregation pathway in a nonpolyphosphate-specific manner. However, because *grlD*⁻ cells

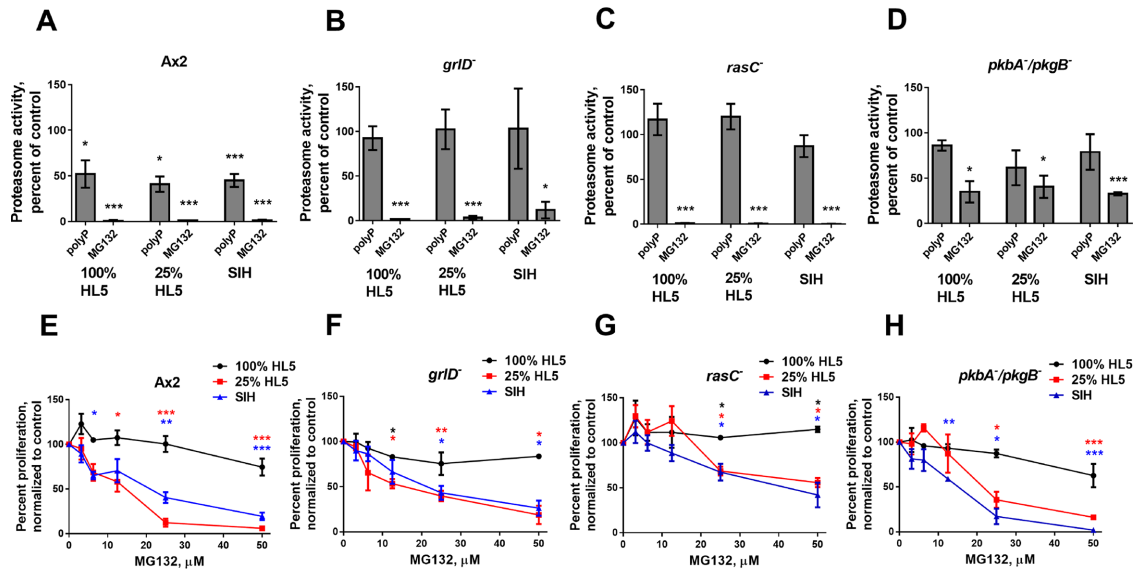


FIGURE 3: Inhibition of proteasome activity inhibits proliferation in low nutrient conditions. (A–D) Cells were cultured in the presence or absence of 150 μM polyphosphate or 25 μM MG132 in the indicated medium for 4 h and proteasome activity levels were measured and normalized to no treatment controls. (E–H) Cells were cultured in the indicated medium at a starting density of 1.5×10^6 cells/ml with the indicated concentrations of MG132. After 24 h, cells were counted, and counts were normalized to the 24-h no MG132 controls. All values are mean \pm SEM, $n \geq 3$. * indicates $p < 0.05$; **, $p < 0.01$; ***, $p < 0.001$ compared with no added polyphosphate or MG132 for the indicated cell type in the indicated medium (paired t tests).

are still responsive to MG132-induced inhibition of proteasome activity but are unresponsive to polyphosphate-induced inhibition of proteasome activity, GrlD does appear to mediate the effects of polyphosphate.

Together, these results suggest that polyphosphate initiates a signaling pathway to inhibit proteasome activity only when cells are at sufficiently high densities, and the resulting proteasome inhibition only leads to proliferation inhibition and entry into development when cells are in low nutrients. Such a mechanism might help prevent premature entry into development, such as when high nutrients are present, or when there are too few cells to effectively aggregate and generate fruiting bodies.

Differential effects of polyphosphate based on nutrient availability

We previously found that proliferation inhibition by polyphosphate affects cytokinesis (cellular division) more than karyokinesis (nuclear division; Suess and Gomer, 2016). Furthermore, we found through proteomic analysis that polyphosphate treated cells showed a decrease in a number of actin/cytoskeleton related proteins (Suess *et al.*, 2017). To further investigate the effects of polyphosphate on the cytoskeleton, we analyzed cell-substratum adhesion and levels of cytoskeletal F-actin and polymerized myosin upon polyphosphate treatment in both high and low nutrient conditions. Polyphosphate caused a decrease in adhesion of cells cultured in 100% HL5 or in SIH, whereas in 25% HL5 polyphosphate had no effect on adhesion (Figure 4, A–C). Cells lacking GrlD were unresponsive to polyphosphate-induced detachment in 100% HL5 or SIH (Figure 4, A–C). Cells lacking either RasC or Akt were sensitive to the effect of polyphosphate on adhesion. We next tested the effect of polyphosphate on levels of cytoskeletal F-actin and polymerized myosin. For wild-type cells in 100% HL5, polyphosphate induced a decrease in F-actin levels, whereas in 25% HL5 polyphosphate increased levels of F-actin (Figure 4, D and E). Polyphosphate had no effect on

cytoskeletal F-actin in SIH (Figure 4F). In 100% HL5, cells lacking GrlD or RasC were unresponsive to the effects of polyphosphate on cytoskeletal F-actin levels (Figure 4D). In 25% HL5, cells lacking GrlD, RasC, or Akt were insensitive to polyphosphate-induced increase in F-actin levels (Figure 4E). Cells lacking GrlD had increased basal levels of cytoskeletal F-actin compared with wild type when cultured in SIH, and cells lacking RasC had increased basal levels of cytoskeletal F-actin in 25% HL5 (Figure 4, E and F). Polyphosphate's effect on cytoskeletal polymerized myosin largely mirrored the effect on F-actin, in that in 100% HL5 polymerized myosin levels decreased, increased in 25% HL5, and were unaltered in SIH (Supplemental Figure S5, A–C). GrlD, RasC, and Akt were all essential for polyphosphate's effect on polymerized myosin in 100 or 25% HL5 (Supplemental Figure S5A). Together, these results suggest that polyphosphate has differential effects on the cell-substratum adhesion and the actin cytoskeleton based on the available nutrients in the microenvironment, and these effects are mediated by the receptor GrlD.

Polyphosphate is essential for efficient aggregation during starvation

Extracellular polyphosphate acts as a prestarvation factor, priming cells for the transition from growth to development in the presence of nutrients (Suess *et al.*, 2017). Starving cells also accumulate extracellular polyphosphate (Suess and Gomer, 2016). To determine the role of polyphosphate during starvation, and to elucidate why *grlD*⁻ cells do not aggregate in submerged stationary cultures (Supplemental Figure S1C), we enzymatically degraded polyphosphate using recombinant exopolyphosphatase (PPX1), an enzyme that degrades polyphosphate from the terminal ends (Wurst and Kornberg, 1994). Starvation causes *Dictyostelium* cells to decrease proteasome activity (Suess *et al.*, 2017). Starved cells treated with PPX1 showed a significant increase in proteasome activity relative to

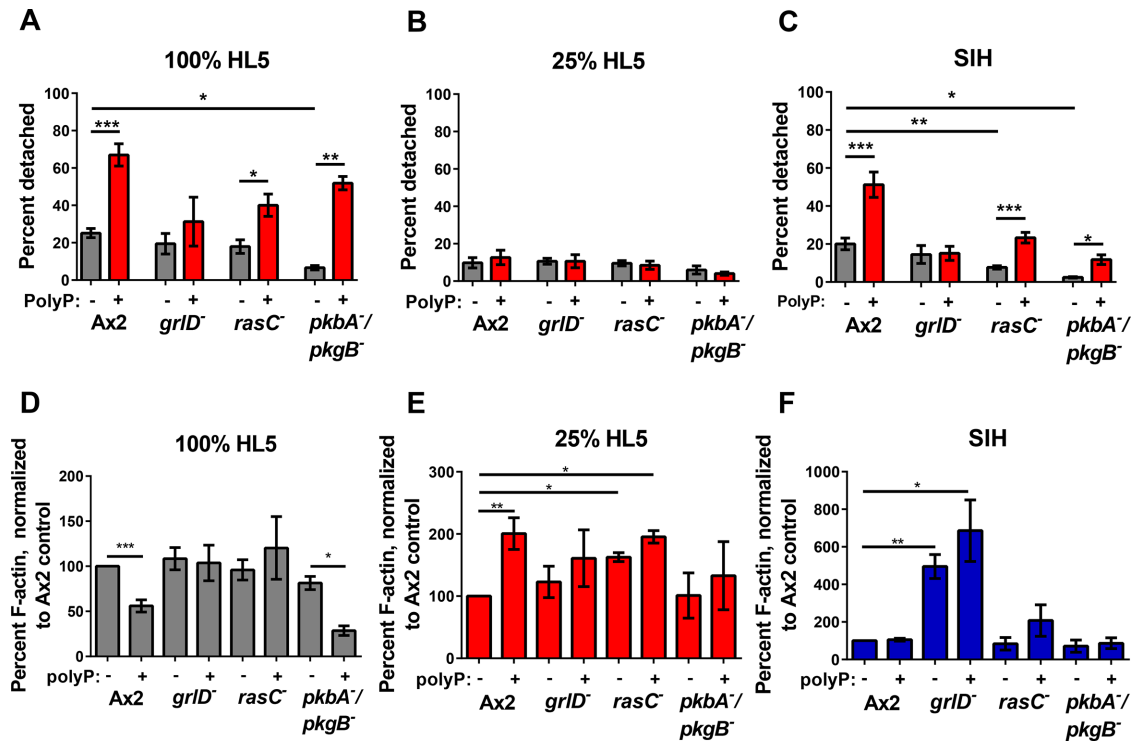


FIGURE 4: Gr1D is necessary for polyphosphate effects on cell-substratum adhesion and actin polymerization. (A–C) Cells were grown in submerged nonshaking cultures in the presence of 150 μ M polyphosphate for 24 h in the indicated medium, then put on an orbital shaker at 70 rpm for 1 h, and attached and detached cell counts were obtained, and the percentage of detached cells was calculated. (D–F) Cells were cultured in 150 μ M polyphosphate for 24 h and cytoskeletal F-actin was measured and normalized to the Ax2 no-polyphosphate control. All values are mean \pm SEM, $n \geq 3$. *, $p < 0.05$; **, $p < 0.01$; ***, $p < 0.001$ (paired t tests).

untreated cells, suggesting that polyphosphate is also involved in proteasome inhibition during starvation (Figure 5A). Because polyphosphate can induce aggregation in the presence of nutrients, we examined the effects of polyphosphate degradation on starvation-induced aggregation for cells in stationary submerged cultures. After 12 h of starvation, untreated cells formed aggregates, and by 24 h the majority of cells were in tightly formed aggregates (Figure 5, B, and C). The addition of PPX1 to starved cells caused a decrease in the formation of aggregates (Figure 5, B and C), similar to the phenotype of *gr1D⁻* cells. Conversely, starved cells treated with 150 μ M exogenous polyphosphate initiated development but formed large unbroken and intricate streaming networks (Figure 5D). Together, these results suggest that polyphosphate is also a signal during starvation-induced development, and that excessively high or low levels of polyphosphate inhibit aggregation.

DISCUSSION

In this article we find that the GPCR Gr1D is essential for the binding of extracellular polyphosphate to *Dictyostelium* cells, and mediates polyphosphate-induced proteasome inhibition and proliferation inhibition. In high nutrient conditions, polyphosphate inhibits proliferation through a mechanism that is not dependent on Gr1D or proteasome inhibition. In low nutrient conditions, polyphosphate inhibits proliferation through a mechanism mediated by Gr1D, RasC, and proteasome inhibition (Figure 6). Cells lacking Gr1D or RasC were unresponsive to polyphosphate proteasome inhibition in all nutrient conditions and polyphosphate proliferation inhibition in low nutrient conditions only. These results suggest that the signal transduction pathways used by polyphosphate to inhibit proliferation are

different depending on nutrient conditions, and that even in high nutrient conditions, polyphosphate primes cells for the eventual transition to development by inhibiting proteasome activity, while the actual transition is held in check by the presence of abundant nutrients.

Cells lacking Gr1D do not respond to polyphosphate-induced aggregation. Although these cells do show an increase in the expression of the aggregation markers CsaA, Car1, and AcaA over time after the induction of starvation, the overall expression levels relative to wild-type cells are significantly lower. Although it is possible that these cells fail to efficiently express the necessary aggregation machinery because of a lack of polyphosphate binding and sensing through Gr1D, it is also possible that Gr1D is necessary for developing aggregation competence regardless of the ability to sense polyphosphate, and so *gr1D⁻* cells fail to respond to polyphosphate-induced aggregation. The mechanism through which this occurs remains ambiguous and warrants a more in-depth analysis; however, it does appear that Gr1D is essential for the development of aggregation competence upon the induction of starvation and the transition to a developmental state.

Polyphosphate-induced aggregation is dependent on cell density, as low-cell-density cultures do not aggregate in the presence of polyphosphate (Suess *et al.*, 2017). Here we find that proteasome inhibition by polyphosphate only occurs at sufficiently high cell densities. These data suggest that this pathway is dependent on cell-cell contact or on the presence of other secreted factors, such as AprA (Brock and Gomer, 2005; Tang *et al.*, 2018).

Polyphosphate inhibits cytokinesis to inhibit proliferation, and cells treated with physiological concentrations of polyphosphate

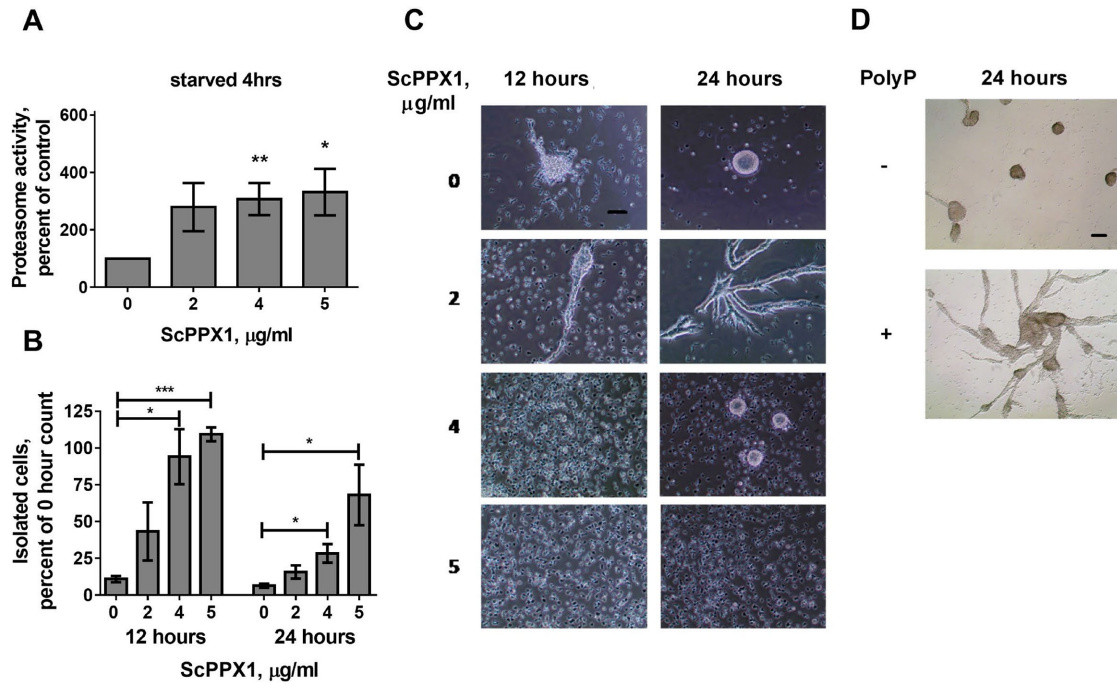


FIGURE 5: Polyphosphate affects starvation-induced development. (A) Cells were starved for 4 h in the indicated concentrations of recombinant exopolyphosphatase, and proteasome activity was measured and normalized to the no exopolyphosphatase control. (B, C) Cells were starved for 24 h in submerged nonshaking culture, and images were taken at 0, 12, and 24 h. The number of cells that were not clearly in an aggregate in $425 \times 425 \mu\text{m}$ fields of view was counted and normalized to the 0 h control. Images in C are representative of seven independent experiments. Bar in C is $50 \mu\text{m}$. (D) Cells were starved in submerged nonshaking culture in the presence or absence of $150 \mu\text{M}$ polyphosphate, and images were taken at 24 h. Images are representative of 10 independent experiments. Bar is $100 \mu\text{m}$. Values in A and B are mean \pm SEM, $n \geq 3$. *, $p < 0.05$; **, $p < 0.01$; ***, $p < 0.001$ (paired t tests).

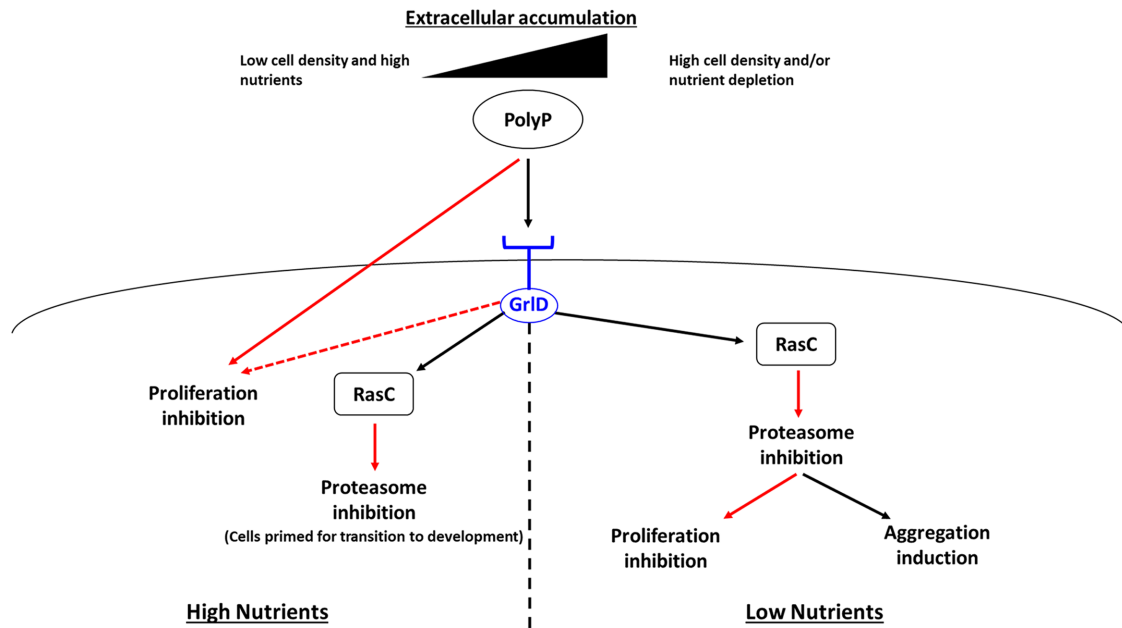


FIGURE 6: Polyphosphate signaling pathway. As cell density increases and/or nutrients are depleted, extracellular polyphosphate accumulation increases. When sufficient extracellular polyphosphate accumulates, it acts as an autocrine signal with the effects dependent on the nutrients available. If nutrients are high, polyphosphate inhibits proliferation through an unknown mechanism. Polyphosphate also inhibits proteasome activation through a pathway facilitated by Gr1D and RasC, priming cells for the eventual transition to development. If nutrients become sufficiently low, polyphosphate inhibits proliferation through a pathway mediated by Gr1D, RasC, and proteasome inhibition. Polyphosphate-induced proteasome inhibition also induces aggregation, the first phase of *Dictyostelium* development. Red arrows indicate inhibition, and the dashed arrow indicates that Gr1D is not essential for proliferation inhibition by polyphosphate in high nutrient conditions.

show a decrease in a number of proteins involved with the actin/cytoskeleton (Suess and Gomer, 2016; Suess *et al.*, 2017). Here we find that polyphosphate affects adhesion and cytoskeletal F-actin and polymerized myosin differentially based on nutrient availability. This shows that in addition to proliferation inhibition and aggregation induction, the effect of polyphosphate on the cytoskeleton is heavily influenced by nutritional status in the microenvironment.

In addition to being accumulated extracellularly during growth, polyphosphate also accumulates during starvation (Suess and Gomer, 2016). We found that starvation induces a decrease in proteasome activity relative to mid-log cells (Suess *et al.*, 2017). Here we found that starved cells treated with recombinant PPK1 have increased proteasome activity levels relative to untreated cells and fail to aggregate efficiently. Starved cells treated with exogenous polyphosphate initiate aggregation, but form large unbroken streaming networks. This suggests that polyphosphate is also an important signal during starvation-induced aggregation. Intracellular polyphosphate also increases in accumulation during starvation and into development (Livermore *et al.*, 2016). Cells lacking the *Dictyostelium* polyphosphate kinase (PPK1) have no detectable intracellular polyphosphate and a decrease in extracellular polyphosphate accumulation at high cell densities (Livermore *et al.*, 2016, Suess and Gomer, 2016). These cells have impaired development including small spore heads and defective germination (Livermore *et al.*, 2016). Both intracellular and extracellular polyphosphate accumulation appear to be essential for *Dictyostelium* development.

Polyphosphate appears to be a cell density-sensing signal that helps cells to be able to predict an imminent starvation and thus increase their fitness before they starve. A high density of *Dictyostelium* cells will eventually outgrow its food source and inevitably starve. Polyphosphate inhibits the proliferation of high-density populations, while still allowing cells to continue to increase nutrient stores (Suess and Gomer, 2016). This would ensure that when nutrients become scarce and development is initiated, the population will have a robust store of accumulated nutrients. By inhibiting the proteasome, polyphosphate might effectively force cells to make do with the available suite of proteins in anticipation of nutrient poverty. Cells at low cell density will have difficulty relaying the cAMP chemoattraction signal, and as a result will form small ineffective fruiting bodies; low concentrations of extracellular polyphosphate might signal to cells that they are at low densities, and push low cell density cells in low nutrients to try to find nutrients rather than initiating development.

Polyphosphate can stabilize and enhance the binding of some ligands to their receptors, such as FGF-1 and FGF-2 to their cell-surface receptors on normal human fibroblasts (Shiba *et al.*, 2003; Kawazoe *et al.*, 2008). There is evidence that polyP signals through the P2Y1 receptor on astrocytes; however, in human umbilical vein endothelial cells polyphosphate can directly bind to histone H4 and HMGB1, which potentially enhances binding to RAGE and P2Y1 receptors (Holmstrom *et al.*, 2013; Dinarvand *et al.*, 2014). We previously found that polyphosphate effects on proliferation and proteasome activity show some conservation between *Dictyostelium* and human cells (Suess *et al.*, 2017). The Gr1D amino acid sequence shows similarity to the G protein-coupled receptor family C member GPR158 of several mammalian species including mice (23% identity) and humans (24% identity). GPR158 is an orphan receptor that is expressed at highest levels in the brain, and is up-regulated in some prostate cancers (Fenner, 2015; Orlandi *et al.*, 2015; Patel *et al.*, 2015). Intriguingly, polyphosphate is also found at high levels in the brain, and can modify amyloidogenic processes (Kumble and Kornberg, 1995; Holmstrom *et al.*, 2013; Cremers *et al.*, 2016). The identification of Gr1D as a mediator of the extracellular polyphos-

phate response in *Dictyostelium* may aid in identifying other polyphosphate signaling pathways in higher eukaryotes.

MATERIALS AND METHODS

Reagents and materials

HL5 and SIH growth media were from Formedium (Norfolk, England). Polyphosphate was from Spectrum (New Brunswick, NJ). Blasticidin, MG132, and proteasome activity assay kits were from MilliporeSigma (Saint Louis, MO). Biotinylated polyphosphate was from KeraFast (Boston, MA). Streptavidin-conjugated Alexa Fluor 647 was from Invitrogen (Carlsbad, CA). Vectors and mutant cell lines were obtained from dictybase.org (Northwestern University). Nylon 17 mm/5 μ m pore size filters were from Sterlitech (Kent, WA).

Strains

Cells used were *Dictyostelium* wild-type Ax2, *pkbA/pkgB*⁻ (DBS0236785), *rasC*⁻ (DBS0236853), and *gr1D*⁻ (DBS0350227). Mutant genotypes were verified by PCR, cells were kept under constant selection, and stocks were never allowed to proliferate above 5×10^6 cells/ml.

Cell culture

Dictyostelium cells were grown at 21°C in shaking culture at 175 rpm in HL5 (10–12 h doubling time) or the synthetic media SIH (~22–26 h doubling time). Proliferation curves used mid-log cells ($[2-4] \times 10^6$ cells/ml), and density was measured every 24 h using a hemocytometer. Percent inhibition was determined by treating control cells as 100% proliferation/0% inhibition, and starting cell density as 0% proliferation/100% inhibition. Doubling times were calculated using the formula $Dt = \text{duration} \times \log(2)/\log(\text{final density}) - \log(\text{initial density})$. Starved cells were cultured in phosphate-buffered medium (PBM) (20 mM KH₂PO₄, 1 mM MgCl₂, 0.01 mM CaCl₂, pH 6.5). Fruiting bodies were generated by plating mid-log cells on a lawn of *Escherichia coli* (Dictybase.org strain DBS0350636) on SM/5 agar plates as defined by Dictybase.org.

Aggregation assay

Mid-log cells were collected by centrifugation at $200 \times g$ for 3 min, resuspended in 25% HL5 (diluted with PBM), SIH, or PBM, and the centrifugation and resuspension were repeated twice. Cells were resuspended to 1.5×10^6 /ml in 25% HL5 and SIH, or 2×10^6 /ml in PBM, and 2 ml was placed in the well of a Falcon 353046 six-well plate (Corning, Corning, NY). Each well had a 9.5 cm² culture area, resulting in 3.2×10^5 cells/cm² for cells in 25% HL5 or SIH, and 3.2×10^5 cells/cm² for cells in PBM. Plates were incubated at room temperature in humid boxes, then examined by microscopy with a 10 \times phase-contrast objective on a Diaphot inverted microscope (Nikon, Garden City, NY) for aggregation and development. Five fields of view from each well were imaged and used to count isolated (unaggregated) cells at appropriate time points. For 0 h images, cells were allowed to adhere for 45 min before images were taken. Images of a calibration slide (SWIFT #MA663; Carlsbad, CA) were used to generate size bars.

Polyphosphate binding assay

Binding of polyphosphate to cells was determined using biotinylated polyphosphate. Cells at mid-log were washed twice with ice-cold PBM and then resuspended in ice-cold PBM. Samples were incubated with biotinylated polyphosphate for 3 min on ice, collected by centrifugation at $200 \times g$ for 3 min at 4°C, then resuspended in ice-cold PBM with streptavidin-conjugated Alexa Fluor 647 (1:200) on ice for 3 min, collected by centrifugation at $200 \times g$

for 3 min at 4°C, and resuspended in ice-cold PBM, and fluorescence was measured using an Accuri C6 flow cytometer (BD Biosciences, San Jose, CA).

Expression of Gr1D in *gr1D*⁻ cells

The *gr1D* cDNA sequence as listed on Dictybase.org was generated and inserted into a cloning vector by GeneArt (Thermo Fischer Scientific). The *gr1D* sequence was inserted into the expression vector pDXA-3C (Manstein *et al.*, 1995) by digesting with *Hind*III (directly preceding the start codon) and *Xho*I (directly after the stop codon) and then ligating. The *gr1D* expression construct was transformed into *Dictyostelium* cells as previously described (Suess and Gomer, 2016), and the resulting transformants were selected with 10 µg/ml G418 until stable colonies were isolated. cDNA from stable transformants were used to assess levels of *gr1D* transcripts using the primers 5'-CGCGAAGCTTATGAAAATTAATTCATT-3' and 5'-CTAATTTCAA-TTCTGGATTATC-3'. The resulting cell line was kept under constant selection using G418. These cells were unable to survive in shaking culture, but did proliferate in axenic media on plastic dishes. To generate enough cells to perform proliferation experiments, 8×10^4 cells were mixed with 0.2 ml of an overnight *E. coli* culture and spread on SM agar plates. After 3–4 d of growth, cells were washed off plates using PBM and washed four times with PBM to remove any residual bacteria. Cells were cultured at 5×10^5 cells/ml in HL5 containing 10 µg/ml G418 for 48 h and then used for the experimental setup.

Filter pad development and discoidin expression

For filter pad development and discoidin staining, 1×10^6 cells were mixed with 0.2 ml of an overnight *E. coli* culture and spread on SM/5 agar plates. After 24 h, cells were harvested as above, collected by centrifugation, and resuspended to 1×10^8 cells/ml. Cells (100 µl) were spotted on Millipore AABP black filters sitting on two layers of PBM-soaked Whatman 3 filter paper, and pads were photographed using a 2× objective. For discoidin staining, cells from the above 10^8 cells/ml stock were diluted to 2×10^6 cells/ml in HL5, and 250 µl was placed in the well of an eight-well slide. Each well had a culture area of 0.83 cm², resulting in 6.0×10^5 cells/cm². After 1 h, 600 µl of 95% EtOH was added to the wells for 10 min, and this was then removed and 500 µl of 95% was added for 10 min to fix the vegetative cells. Other slides contained cells similarly diluted in PBM and were fixed after 2 h. After air drying, cells were rehydrated for 1 h with PBS/0.02% Tween-20 (PBST). Cells were stained with 0.66 µg/ml mouse immunoglobulin G1 (IgG1) anti-discoidin I (Developmental Studies Hybridoma Bank 80-52-13; Bertholdt *et al.*, 1985) or 0.66 µg/ml irrelevant mouse IgG1 (Biolegend) in PBST for 1 h, washed three times for 5 min each in PBST, incubated for 1 h with 1:500 Alexa 488 F(ab')₂ donkey-anti-mouse IgG (Jackson) in PBST, washed as above, and mounted with Vectashield (Vector Laboratories). A 1 mm standard slide with 10 µm rulings was used for size calibration.

qPCR and semiquantitative RT-PCR

Ax2 (3×10^5) or *gr1D*⁻ cells were mixed with ~20 µl of *E. coli* from a LB plate, and this was spread on a SM/5 plate. After 36 h, the cells were collected in 15 ml of ice-cold water and the *Dictyostelium* cells were collected by centrifugation at $400 \times g$ for 5 min. Cells were resuspended in water and washed by centrifugation, and the pellet was resuspended to 1×10^8 cells/ml in PBM. Cells (50 µl) were used for the 0 h time point. For developmental time points, cells (50 µl) were spotted on AABP black filter pads following Phillips and Gomer (2010) and at the indicated times cells were washed off the pad with 1 ml of PBM and collected by centrifugation. RNA at each time point was extracted using a Quick-RNA kit (R1054; Zymo

Research, Irvine, CA) and then the cDNA library was synthesized using the RNA as a template with a cDNA synthesis kit (K1651; Thermo Fisher Scientific). qPCR was done using the cDNA library with the primers for *gapdh* forward 5'-ACCGTTCACGCCATCACT-GCC-3' and reverse 5'-GACGGACGGTTAAATCGACGACTG-3', for *csaA* forward 5'-CACACCAACCAATGTAACCGTC-3' and reverse 5'-AGGTTTGGTGGCCTTGAGGT-3', for *car1* forward 5'-AGTGT-CAATGGTGGTTCCCT-3' and reverse 5'-CAACCAATACTGCT-GAAATTGCCCA-3', and for *acaA* forward 5'-TGGTCCTTTGGT-GCTGGTTG-3' and reverse 5'-GGTGAGGCAATACCAGCAGGA-3'. Data were acquired with a QuantStudio 6 Flex real-time PCR system and analyzed by QuantStudio Software V1.3. Conventional PCR was done using the same cDNA library and primers, and the PCR product was run on a 1% agarose-TAE gel with ethidium bromide. The gel image was taken with a Bio-Rad ChemiDoc XRS+ imaging system and the band intensity was determined by ImageLab software. The intensity ratio (target gene vs. *gapdh*) was then normalized to the AX2 time 0 sample. AzuraView GreenFast qPCR blue mix (AZ-2305; Azura Genomics) and Azura 2× HS Taq Red Mix (AZ-1622; Azura Genomics) were used for qPCR and conventional PCRs.

Proteasome activity assay

Cells from mid-log cultures ($[2-4] \times 10^6$ /ml) were washed twice in HL5, 25% HL5, or SIH, and resuspended in HL5, 25% HL5, or SIH containing polyphosphate or Mg132. After 4 h, 1×10^6 cells were collected by centrifugation at $200 \times g$ for 3 min and resuspended in 400 µl of PBS. Cell lysates were generated by passing cells through 5 µm pore size syringe filters. Cell lysate (100 µl) was incubated with 100 µl of proteasome activity kit assay buffer, which contains a fluorescence indicator for proteasome complex activity that upon cleavage produces strong green fluorescence. Samples were incubated at room temperature overnight in the dark, and fluorescence was measured with an excitation of 490 nm and emission of 525 nm using a Synergy Mx plate reader (BioTek, Winooski, VT).

Adhesion assay

Adhesion assays were performed as described in Fey *et al.* (2002) with the following modifications. Cells were plated at 1.5×10^6 cells/ml in 2 ml (six-well plate, 9.5 cm² culture area/well; resulting in 3.2×10^5 cells/cm²) with 150 µM polyP or an equal volume of buffer and incubated overnight at room temperature. The next day dishes were placed on an orbital shaker set to 70 rpm for 1 h. Detached cells were removed by pipetting off the plate and counted using a hemocytometer. To count attached cells, 2 ml of fresh media was used to thoroughly wash the attached cells off the dish and these were counted using a hemocytometer. The percent of detached cells was calculated as (detached cells/[attached + detached cells]) × 100.

F-actin and polymerized myosin assays

F-actin and polymerized myosin II were quantified as in Uyemura *et al.* (1978) with the following modifications. Mid-log cells were plated at 1.5×10^6 cells/ml in 2 ml of the appropriate medium with 150 µM polyP or an equal volume of buffer in six-well dishes. Cells were incubated in a humid box at room temperature for 24 h and then counted. Cells (1×10^6) were collected by centrifugation at $200 \times g$ for 3 min and resuspended in lysis buffer (100 mM PIPES [pH 6.8], 1 mM MgCl₂, 2.5 mM ethylene glycol-bis(β-aminoethyl ether)-*N,N,N',N'*-tetraacetic acid [EGTA], 10 mM *N*-*p*-tosyl-L-arginine methyl ester hydrochloride [TAME], 0.5% Triton X-100) containing protease and phosphatase inhibitor cocktail (Cell Signaling; 5872S). Samples were inverted five times and incubated on ice.

After 3 min, detergent insoluble cytoskeletons were collected by centrifugation at 15,000 × g for 8 min at 4°C. The supernatant was discarded and the pellet was resuspended in lysis buffer and mixed thoroughly, and then cytoskeletons were collected by centrifugation at 15,000 × g for 8 min at 4°C. The pellet was then resuspended in SDS sample buffer containing protease and phosphatase inhibitor cocktail and incubated at 95°C for 5 min. Samples were run on 4–20% polyacrylamide gels (Bio-Rad; 4561093), and then stained with Coomassie blue for 1 h, and destained for 2 h. Gels were imaged with a ChemiDoc XRS+ (Bio-Rad, Hercules, CA) and quantification of actin and myosin II bands was determined with Image Lab (Bio-Rad).

Enzymatic treatments

The plasmid for purifying yeast PPX1 was kindly provided by Michael Gray (University of Alabama at Birmingham; Gray et al., 2014). Recombinant protein purification was performed as previously described (Brock and Gomer, 2005). For ScPPX1 treatment of cell cultures, cells were inoculated with ScPPX1 or an equal volume of buffer.

Statistics

Statistical analysis was performed using Prism (GraphPad, San Diego, CA). Differences between two groups were assessed by Student's t test. Differences between multiple groups were assessed by one-way analysis of variance using Tukey's posttest. Significance was defined as $p < 0.05$.

ACKNOWLEDGMENTS

We thank Yuantai Wu and Chris Janetopoulos for the gift of the *grlD*⁻ cells, Michael Gray for the expression plasmid for purifying yeast PPX1, Ramesh Rijal for help with cell culture, Tejas Karhadkar for help with photography, Ramesh Rijal for helpful comments, and Dictybase for the cell lines. This work was supported by National Institutes of Health R01 Grant no. GM-102280.

REFERENCES

Achbergerova L, Nahalka J (2011). Polyphosphate—an ancient energy source and active metabolic regulator. *Microb Cell Fact* 10, 63.

Ardeshyrlajimi A, Golchin A, Khojasteh A, Bandehpour M (2018). Increased osteogenic differentiation potential of MSCs cultured on nanofibrous structure through activation of Wnt/ β -catenin signalling by inorganic polyphosphate. *Artif Cells Nanomed Biotechnol* 46, 1–7.

Auesukaree C, Tochio H, Shirakawa M, Kaneko Y, Harashima S (2005). Plc1p, Arg82p, and Kcs1p, enzymes involved in inositol pyrophosphate synthesis, are essential for phosphate regulation and polyphosphate accumulation in *Saccharomyces cerevisiae*. *J Biol Chem* 280, 25127–25133.

Bertholdt G, Stadler J, Bozzaro S, Fichtner B, Gerisch G (1985). Carbohydrate and other epitopes of the contact site A glycoprotein of *Dictyostelium discoideum* as characterized by monoclonal antibodies. *Cell Differ* 16, 187–202.

Brock DA, Gomer RH (2005). A secreted factor represses cell proliferation in *Dictyostelium*. *Development* 132, 4553–4562.

Brown MR, Kornberg A (2004). Inorganic polyphosphate in the origin and survival of species. *Proc Natl Acad Sci USA* 101, 16085–16087.

Cremers CM, Knoefler D, Gates S, Martin N, Dahl JU, Lempart J, Xie L, Chapman MR, Galvan V, Southworth DR, Jakob U (2016). Polyphosphate: a conserved modifier of amyloidogenic processes. *Mol Cell* 63, 768–780.

Daniel J, Bush J, Cardelli J, Spiegelman GB, Weeks G (1994). Isolation of two novel ras genes in *Dictyostelium discoideum*; evidence for a complex, developmentally regulated ras gene subfamily. *Oncogene* 9, 501–508.

Dinarvand P, Hassanian SM, Qureshi SH, Manithody C, Eissenberg JC, Yang L, Rezaie AR (2014). Polyphosphate amplifies proinflammatory responses of nuclear proteins through interaction with receptor for

advanced glycation end products and P2Y1 purinergic receptor. *Blood* 123, 935–945.

Fenner A (2015). Prostate cancer: orphan receptor GPR158 finds a home in prostate cancer growth and progression. *Nat Rev Urol* 12, 182.

Fey P, Stephens S, Titus MA, Chisholm RL (2002). SadA, a novel adhesion receptor in *Dictyostelium*. *J Cell Biol* 159, 1109–1119.

Frazier WA, Rosen SD, Reitherman RW, Barondes SH (1975). Purification and comparison of two developmentally regulated lectins from *Dictyostelium discoideum*. Discoidin I and II. *J Biol Chem* 250, 7714–7721.

Ghosh S, Shukla D, Suman K, Lakshmi BJ, Manorama R, Kumar S, Bhandari R (2013). Inositol hexakisphosphate kinase 1 maintains hemostasis in mice by regulating platelet polyphosphate levels. *Blood* 122, 1478–1486.

Ginsburg GT, Gollop R, Yu Y, Louis JM, Saxe CL, Kimmel AR (1995). The regulation of *Dictyostelium* development by transmembrane signalling. *J Eukaryot Microbiol* 42, 200–205.

Gray MJ, Jakob U (2015). Oxidative stress protection by polyphosphate—new roles for an old player. *Curr Opin Microbiol* 24, 1–6.

Gray MJ, Wholey WY, Wagner NO, Cremers SH, Mueller-Schickert A, Hock NT, Krieger AG, Smith EM, Bender RA, Bardwell JC, Jakob U (2014). Polyphosphate is a primordial chaperone. *Mol Cell* 53, 689–699.

Heidel AJ, Lawal HM, Felder M, Schilde C, Helps NR, Tunggal B, Rivero F, John U, Schleicher M, Eichinger L, et al. (2011). Phylogeny-wide analysis of social amoeba genomes highlights ancient origins for complex intercellular communication. *Genome Res* 21, 1882–1891.

Holmstrom KM, Marina N, Baev AY, Wood NW, Gourine AV, Abramov AY (2013). Signalling properties of inorganic polyphosphate in the mammalian brain. *Nat Commun* 4, 1362.

Kato K, Morita K, Hirata I, Doi K, Kubo T, Kato K, Tsuga K (2018). Enhancement of calcification by osteoblasts cultured on hydroxyapatite surfaces with adsorbed inorganic polyphosphate. *In Vitro Cell Dev Biol Anim* 54, 449–457.

Kawano MM (2006). Inorganic polyphosphate induces apoptosis specifically in human plasma cells. *Haematologica* 91, 1154a.

Kawazoe Y, Katoh S, Onodera Y, Kohgo T, Shindoh M, Shiba T (2008). Activation of the FGF signaling pathway and subsequent induction of mesenchymal stem cell differentiation by inorganic polyphosphate. *Int J Biol Sci* 4, 37–47.

Kulakovskaya T (2018). Inorganic polyphosphates and heavy metal resistance in microorganisms. *World J Microbiol Biotechnol* 34, 139.

Kumble KD, Kornberg A (1995). Inorganic polyphosphate in mammalian cells and tissues. *J Biol Chem* 270, 5818–5822.

Livermore TM, Chubb JR, Saiardi A (2016). Developmental accumulation of inorganic polyphosphate affects germination and energetic metabolism in *Dictyostelium discoideum*. *Proc Natl Acad Sci USA* 113, 996–1001.

Loomis WF (2014). Cell signaling during development of *Dictyostelium*. *Dev Biol* 391, 1–16.

Lu Y, Knol JC, Linskens MH, Friehs K, van Haastert PJ, Flaschel E (2004). Production of the soluble human Fas ligand by *Dictyostelium discoideum* cultivated on a synthetic medium. *J Biotechnol* 108, 243–251.

Manstein DJ, Schuster HP, Morandini P, Hunt DM (1995). Cloning vectors for the production of proteins in *Dictyostelium discoideum*. *Gene* 162, 129–134.

Meili R, Ellsworth C, Firtel RA (2000). A novel Akt/PKB-related kinase is essential for morphogenesis in *Dictyostelium*. *Curr Biol* 10, 708–717.

Morrissey JH, Choi SH, Smith SA (2012). Polyphosphate: an ancient molecule that links platelets, coagulation, and inflammation. *Blood* 119, 5972–5979.

Noegel A, Gerisch G, Stadler J, Westphal M (1986). Complete sequence and transcript regulation of a cell adhesion protein from aggregating *Dictyostelium* cells. *EMBO J* 5, 1473–1476.

Orlandi C, Xie K, Masuho I, Fajardo-Serrano A, Lujan R, Martemyanov KA (2015). Orphan receptor GPR158 is an allosteric modulator of RGS7 catalytic activity with an essential role in dictating its expression and localization in the brain. *J Biol Chem* 290, 13622–13639.

Ozeki N, Hase N, Yamaguchi H, Hiyama T, Kawai R, Kondo A, Nakata K, Mogi M (2015). Polyphosphate induces matrix metalloproteinase-3-mediated proliferation of odontoblast-like cells derived from induced pluripotent stem cells. *Exp Cell Res* 333, 303–315.

Patel N, Itakura T, Jeong S, Liao CP, Roy-Burman P, Zandi E, Groshen S, Pinski J, Coetzee GA, Gross ME, Fini ME (2015). Expression and functional role of orphan receptor GPR158 in prostate cancer growth and progression. *PLoS One* 10, e0117758.

- Phillips JE, Gomer RH (2010). The ROCO kinase QkgA is necessary for proliferation inhibition by autocrine signals in *Dictyostelium discoideum*. *Eukaryot Cell* 9, 1557–1565.
- Pitt GS, Milona N, Borleis J, Lin KC, Reed RR, Devreotes PN (1992). Structurally distinct and stage-specific adenylyl cyclase genes play different roles in *Dictyostelium* development. *Cell* 69, 305–315.
- Prabhu Y, Eichinger L (2006). The *Dictyostelium* repertoire of seven transmembrane domain receptors. *Eur J Cell Biol* 85, 937–946.
- Rao NN, Gomez-Garcia MR, Kornberg A (2009). Inorganic polyphosphate: essential for growth and survival. *Annu Rev Biochem* 78, 605–647.
- Rao NN, Kornberg A (1996). Inorganic polyphosphate supports resistance and survival of stationary-phase *Escherichia coli*. *J Bacteriol* 178, 1394–1400.
- Rashid MH, Rumbaugh K, Passador L, Davies DG, Hamood AN, Iglewski BH, Kornberg A (2000). Polyphosphate kinase is essential for biofilm development, quorum sensing, and virulence of *Pseudomonas aeruginosa*. *Proc Natl Acad Sci USA* 97, 9636–9641.
- Rock KL, Gramm C, Rothstein L, Clark K, Stein R, Dick L, Hwang D, Goldberg AL (1994). Inhibitors of the proteasome block the degradation of most cell proteins and the generation of peptides presented on MHC class I molecules. *Cell* 78, 761–771.
- Shiba T, Nishimura D, Kawazoe Y, Onodera Y, Tsutsumi K, Nakamura R, Ohshiro M (2003). Modulation of mitogenic activity of fibroblast growth factors by inorganic polyphosphate. *J Biol Chem* 278, 26788–26792.
- Smith SA, Mutch NJ, Baskar D, Rohloff P, Docampo R, Morrissey JH (2006). Polyphosphate modulates blood coagulation and fibrinolysis. *Proc Natl Acad Sci USA* 103, 903–908.
- Soll DR, Yarger J, Mirick M (1976). Stationary phase and the cell cycle of *Dictyostelium discoideum* in liquid nutrient medium. *J Cell Sci* 20, 513–523.
- Suess PM, Gomer RH (2016). Extracellular polyphosphate inhibits proliferation in an autocrine negative feedback loop in *Dictyostelium discoideum*. *J Biol Chem* 291, 20260–20269.
- Suess PM, Watson J, Chen W, Gomer RH (2017). Extracellular polyphosphate signals through Ras and Akt to prime *Dictyostelium discoideum* cells for development. *J Cell Sci* 130, 2394–2404.
- Tang Y, Wu Y, Herlihy SE, Brito-Aleman FJ, Ting JH, Janetopoulos C, Gomer RH (2018). An autocrine proliferation repressor regulates *Dictyostelium discoideum* proliferation and chemorepulsion using the G protein-coupled receptor GrhH. *MBio* 9, e02443-17.
- Uyemura DG, Brown SS, Spudich JA (1978). Biochemical and structural characterization of actin from *Dictyostelium discoideum*. *J Biol Chem* 253, 9088–9096.
- Wang L, Fraley CD, Faridi J, Kornberg A, Roth RA (2003). Inorganic polyphosphate stimulates mammalian TOR, a kinase involved in the proliferation of mammary cancer cells. *Proc Natl Acad Sci USA* 100, 11249–11254.
- Werner TP, Amrhein N, Freimoser FM (2007a). Inorganic polyphosphate occurs in the cell wall of *Chlamydomonas reinhardtii* and accumulates during cytokinesis. *BMC Plant Biol* 7, 51.
- Werner TP, Amrhein N, Freimoser FM (2007b). Specific localization of inorganic polyphosphate (poly P) in fungal cell walls by selective extraction and immunohistochemistry. *Fungal Genet Biol* 44, 845–852.
- Wurst H, Kornberg A (1994). A soluble exopolyphosphatase of *Saccharomyces cerevisiae*. Purification and characterization. *J Biol Chem* 269, 10996–11001.